Journal of Anatomy

J. Anat. (2011) **219**, pp388–402 doi: 10.1111/j.1469-7580.2011.01402.x

Effects of growth on geometry of gastrocnemius muscle in children: a three-dimensional ultrasound analysis

Menno R. Bénard,[1,2] Jaap Harlaar,[2] Jules G. Becher,[2] Peter A. Huijing[1] and Richard T. Jaspers[1]

[1]*Research Institute Move, Faculty of Human Movement Sciences, VU University, Amsterdam, the Netherlands*
[2]*Department of Rehabilitation Medicine, Research Institute Move, VU University Medical Center, Amsterdam, the Netherlands*

Abstract

During development, muscle growth is usually finely adapted to meet functional demands in daily activities. However, how muscle geometry changes in typically developing children and how these changes are related to functional and mechanical properties is largely unknown. In rodents, longitudinal growth of the pennate m. gastrocnemius medialis (GM) has been shown to occur mainly by an increase in physiological cross-sectional area and less by an increase in fibre length. Therefore, we aimed to: (i) determine how geometry of GM changes in healthy children between the ages of 5 and 12 years, (ii) test whether GM geometry in these children is affected by gender, (iii) compare normalized growth of GM geometry in children with that in rats at similar normalized ages, and (iv) investigate how GM geometry in children relates to range of motion of angular foot movement at a given moment. Thirty children (16 females, 14 males) participated in the study. Moment-angle data were collected over a range of angles by rotating the foot from plantar flexion to dorsal flexion at standardized moments. GM geometry in the mid-longitudinal plane was measured using three-dimensional ultrasound imaging. This geometry was compared with that of GM geometry in rats. During growth from 5 to 12 years of age, the mean neutral footplate angle (0 Nm) occurred at −5° (SD 7°) and was not a function of age. Measured at standardized moments (4 Nm), footplate angles towards plantar flexion and dorsal flexion decreased by 25 and 40%, respectively. In both rats and children, GM muscle length increased proportionally with tibia length. In children, the length component of the physiological cross-sectional area and fascicle length increased by 7 and 5% per year, respectively. Fascicle angle did not change over the age range measured. In children, the Achilles tendon length increased by 6% per year. GM geometry was not affected by gender. We conclude that, whereas the length of GM in rat develops mainly by an increase in physiological cross-sectional area of the muscle, GM in children develops by uniform scaling of the muscle. This effect is probably related to the smaller fascicle angle in human GM, which entails a smaller contribution of radial muscle growth to increased GM muscle length. The net effect of uniform scaling of GM muscle belly causes it to be stiffer, explaining the decrease in range of motion of angular foot movement at 4 Nm towards dorsal flexion during growth.

Key words: children; development; gastrocnemius medialis; growth; hypertrophy; muscle; muscle geometry; ultrasound imaging.

Introduction

In pennate muscles, the major determinants of muscle function are the number of muscle fibres, the muscle fibre cross-sectional area, the number of sarcomeres in series, the organization of fibres within the muscle and the connective tissue properties. During development, these characteristics are usually finely adapted to meet the functional demands in daily activities. During growth, the muscle needs to grow to keep up with the increase in body mass and bone length. However, in congenital and hereditary neuromuscular disorders such as cerebral palsy and brachial plexus injury, muscle growth is hampered and, consequently, joint mobility is limited (Tardieu et al. 1982; Shortland et al. 2002; Van Gelein Vitringa et al. 2011). Improvement of treatment of

Correspondence
Menno R. Bénard, Research Institute Move, Faculty of Human Movement Sciences, VU University, Amsterdam, the Netherlands.
E: m.r.benard@vu.nl

Accepted for publication *12 May 2011*
Article published online *2 June 2011*

the affected developing muscle requires a detailed insight into how its geometry develops and how this differs from that of typically developing muscle.

To date, very little is known about the development of the geometry of a typically developing muscle (Blazevich & Sharp, 2005). The few studies available indicate that both pennation angle (Binzoni et al. 2001; Narici et al. 2003; Kawakami et al. 2006; Thom et al. 2007; Mademli & Arampatzis, 2008; Morse et al. 2008b) and fascicle length (Mohagheghi et al. 2008) increase with age, although a lack of correlation of these variables with age has also been reported (Legerlotz et al. 2010). Furthermore, the functional implications of these results are unknown, as the changes in variables are not related to functional or mechanical variables. To the best of our knowledge, a comprehensive study of how the major determinants of the muscle length–force characteristics change with age has not been performed.

Muscle geometry during development has been extensively studied in rodents. These studies showed an increase in pennation angle (Stickland, 1983; m. soleus) and showed that the longitudinal growth of the muscle (belly), specifically in the m. gastrocnemius medialis (GM), is due predominantly to an increase in physiological cross-sectional area of the muscle and not to an increase in fibre length by addition of sarcomeres in series (De Koning et al. 1987; Heslinga & Huijing, 1990, 1993). The question is raised whether muscle growth of children in the same relative age is similar to that in rodents.

The aims of our study were to: (i) determine how geometry of GM changes in children at the ages from 5 to 12 years, (ii) test whether GM geometry in these children is influenced by gender, (iii) compare growth of GM geometry in children with that in rats; (iv) investigate how GM geometry in children relates to range of motion of angular foot movement.

Our main hypothesis is that, in children, the longitudinal growth of GM muscle belly in the mid-longitudinal plane is due to an increase in the length component of the physiological cross-sectional area of the muscle and not to an increase in fascicle length.

A widely used visualizing technique for studying muscles *in vivo* is free-hand two-dimensional (2-D) ultrasound. With this technique, valid measurements of the muscle geometry can be obtained (i.e. Kawakami et al. 1993; Benard et al. 2009). A recent development in this field of research is the extension from 2- to 3-D ultrasound (Fry et al. 2004; Kurihara et al. 2005; Barber et al. 2009). As 3-D ultrasound allows valid measurements in the mid-longitudinal plane and of the muscle belly length (Barber et al. 2009), this technique will be used to measure muscle geometry of GM in children. For a comparison with GM geometry in rats, data from previous *in situ* studies of rat GM performed by Huijing and co-workers will be re-analyzed (De Koning et al. 1987; Heslinga & Huijing, 1990, 1993).

Materials and methods

Subjects

Thirty children (16 female and 14 male Caucasians aged 5–12 years) participated in the study after obtaining informed consent from their parents. The study was approved by the Medical Ethics Committee of the VU University Medical Centre.

Anthropometry

The whole protocol was executed by one investigator. For all children, the right leg was studied. To allow left/right comparisons, the whole protocol was repeated on the left leg in 15 of these children as well. Body mass, tibia length ($\ell_{(tib)}$) and Achilles tendon moment arm were measured. Tibia length was calculated as the mean of the distance from the tibia plateau to the most prominent part of the malleoli, measured on both the lateral and the medial side of the leg. Within the sagittal plane, Achilles tendon moment arm length was calculated as the mean of the smallest distance from these most prominent parts of the malleoli to the middle of the Achilles tendon, measured on both lateral and medial sides of the leg. This length was measured at a foot angle of 0° (defined as the angle with lateral border of the foot sole perpendicular to the tibia).

Footplate moment-angle data

For subsequent measurements, the children were lying prone on a bench, with both feet overhanging the edge. To measure foot angle at standardized moments in the children, a custom-designed hand-held dynamometer was used (Benard et al. 2010). The hand-held dynamometer consists of an adjustable foot-fixation, a torque wrench and a goniometer (Fig. 1A). The foot-fixation has a part for the forefoot and a part for the calcaneus that can both be adjusted for a good fit. Both parts are fastened to the foot using Velcro straps. At its connection with the foot-fixation, the torque wrench is used to measure the moment within the sagittal plane (i.e. towards dorsal flexion and plantar flexion). The angle of the footplate with the horizontal was measured using the goniometer placed on the torque wrench (Fig. 1A). Moment (Nm) and angle (°) are read out simultaneously. For both variables, positive values refer to dorsal flexion conditions.

Footplate angle and moment data were collected at: (i) the angle corresponding to a moment of −4 Nm (φ_{plant}), (ii) the angle corresponding to a moment of 0 Nm (φ_{neutr}), (iii) the angle corresponding to a moment of 4 Nm (φ_{dors}), (iv) the moment at an angle halfway between angles i and ii, and (v) the moment at the angle halfway between angles ii and iii. Moments higher than 4 Nm caused discomfort in the children and decreased the ability to relax (e.g. higher EMG activity). In addition, in pilot work, exerting such a higher moment (up to a maximum of 7 Nm) yielded angles within 5° of those measured at 4 Nm. All dynamometer measurements were repeated five times and for each repetition the moment applied was held for 5 s (Benard et al. 2010). The mean result of five repetitions taken at the end of 5 s holding time was taken as a data point.

From the moment-angle data, the slope of the moment-angle curve was calculated towards both dorsal flexion (m_{dors}) and

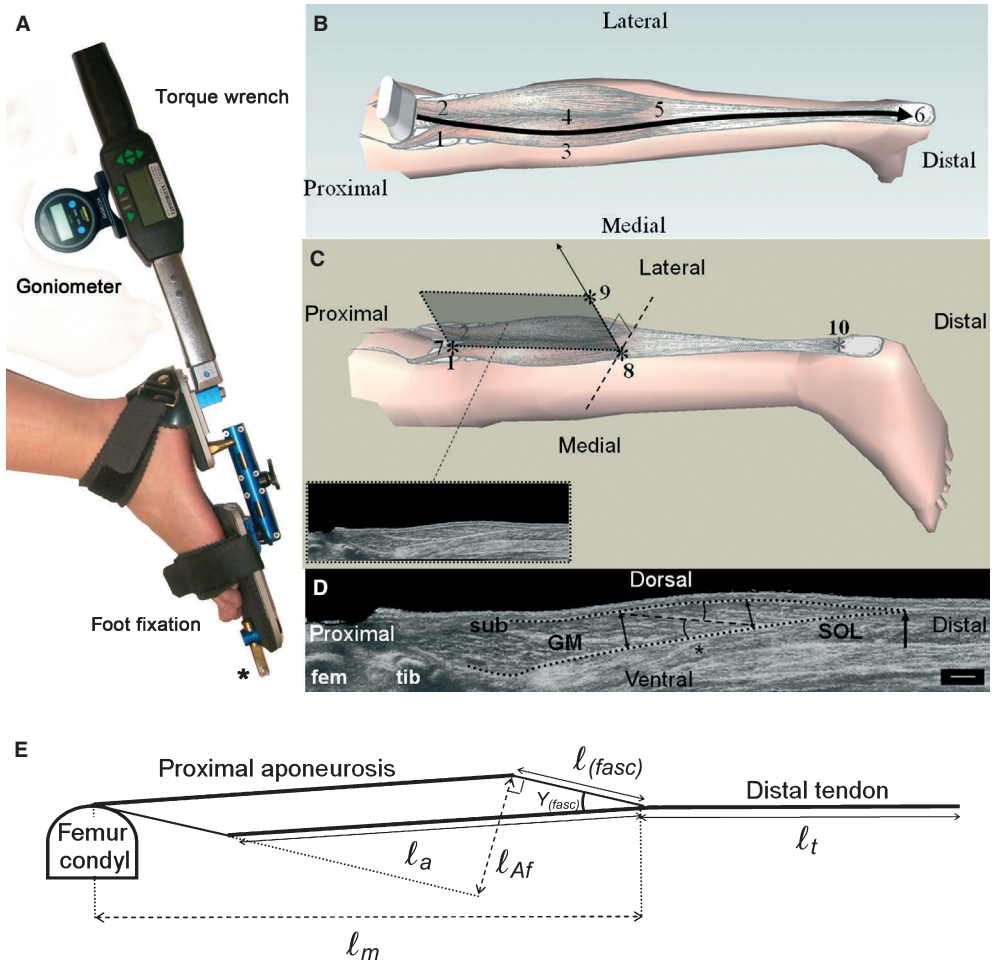

Fig. 1 Schematics of the hand-held dynamometer, 3-D ultrasound imaging protocol and measurement of GM geometry. (A) The hand-held dynamometer consists of an adjustable foot-fixation, a torque wrench and a goniometer. The foot-fixation has parts supporting the forefoot and calcaneus. These parts are connected by a rod, allowing independent adjustments in rotation and abduction/adduction. The forefoot part is equipped with a fixation point to the table (*). (B) An example of the path of the ultrasound probe during a scanning of GM following guide marks, from proximal to distal: (1) the medial and (2) lateral condyl of the femur, (3) the medial and (4) lateral border of GM muscle belly, (5) the most distal muscle belly end and (6) the calcaneus. (C) Three orientation items (*) were used to define the mid-longitudinal plane of GM (shaded plane and inset). (7) The estimate of the origin of GM (for definition, see Materials and methods and also see markers 1 and 2 in B), (8) the most distal muscle belly end, and (9) a line perpendicular to tangent to the distal aponeurosis in the transversal plane (dotted line). A marker was placed at (10) the ventral intersection of the Achilles tendon and the calcaneus to measure tendon length. (D) Measurement of muscle geometry of GM within its mid-longitudinal plane. GM is covered by the subcutis (SUB) and supported by m. soleus (SOL). Parts of both femur (fem) and tibia (tib) are shown. The black dotted lines define the outline of the muscle. The most distal muscle belly end is indicated by a black arrow. The length of the target fascicle $\ell_{(fasc)}$ (dashed black line), centred at two-thirds (*) of muscle belly length (from the origin) is measured. Muscle thickness was calculated as the mean of the thicknesses at the ends (black double arrows) of the target fascicle. The fascicle–aponeurosis angle was also calculated as the mean of the angles of the fascicle with the proximal and distal aponeurosis (black arcs). Scale bar: 1 cm. (E) Model of the mid-longitudinal plane from which the length of the aponeurosis (ℓ_a) and the length component of the physiological cross-sectional area (ℓ_{Af}) were calculated (see text for details).

plantar flexion (m_{plant}). Linear estimates of joint stiffness were calculated for overall comparative means, according to Eqs 1 and 2:

$$m_{dors} = \frac{4}{\text{dorsal angle} - \text{neutral angle}} [\text{Nm per degree}] \quad (1)$$

$$m_{plant} = \frac{-4}{\text{plantar angle} - \text{neutral angle}} [\text{Nm per degree}] \quad (2)$$

3-D ultrasound imaging of m. gastrocnemius medialis

A 3-D ultrasound reconstruction of m. gastrocnemius medialis (GM) was made at three muscle length conditions, corresponding to the footplate angles φ_{plant}, φ_{neutr} and φ_{dors}. For each condition, the footplate was fixed via the foot-fixation (Fig. 1A). Transverse ultrasound scans of GM were made dynamically using a B-mode ultrasound device (Technos MPX, Esaote S.p.A., Italy) with a 5-cm linear array probe (12.5 MHz).

The ultrasound images were recorded at 25 Hz using a video card (miroVIDEO DC30; Pinnacle Systems Inc.). The ultrasound scans were done as follows. The scanning area was covered with a thick layer of ultrasound gel (5 mm) to minimize necessary pressure exerted by the probe on the skin and to improve image quality. The ultrasound probe was moved with a transverse orientation, starting proximal to the femur condyles and ending at the most dorsal part of the calcaneus (Fig. 1B). This movement was guided by markers indicating the lateral and medial condyle of the femur, the lateral and medial borders of the muscle belly, the distal muscle belly end and the calcaneus (see markers #1–6 in Fig. 1B). On average, a scan took about 30 s. The position and orientation of the ultrasound probe were recorded at a frequency of 25 Hz by tracking a three-marker frame, rigidly attached to the probe, using a one-camera Optotrak 3020 system (Northern Digital, Waterloo, Canada).

Prior to executing the protocol, the setup was calibrated by tracking, within the ultrasound image, a cross-point of two wires located in a water cube whilst moving the ultrasound probe around the cross-point (Prager et al. 1998). By using a least-squares fit on the cross-section in the collected ultrasound images, the system was calibrated spatially for three translations and three rotations. Using the calibration, the 3-D positions of the pixels within ultrasound images were calculated using software custom programmed in MATLAB (version 7.1; the Mathworks Inc.). With the software, a digital reconstruction of the scanned area of GM was created using a nearest neighbour algorithm on the pixels in the collected ultrasound images (Gee et al. 2004).

Electromyography

To control for involuntary activation during the dynamometer and ultrasound protocol, electromyographic (EMG) signals of m. tibialis anterior and m. gastrocnemius lateralis were A/D converted at 1000 Hz using a multichannel system (Porti5, TMS-International™, the Netherlands) and recorded on a PC. Skin preparation and electrode placement of EMG were carried out according to SENIAM guidelines (Freriks et al. 1999). For each muscle, two electrodes were placed 2 cm apart longitudinally (centre to centre) at the most prominent middle portion of the muscle bellies. Before the measurements, EMG at maximal voluntary contraction (MVC) of about 5 s was measured in prone position for both muscles at 0° footplate angle. EMG signals were off-line full-wave rectified, high-pass filtered at 20 Hz to remove artefacts, and subsequently normalized to the peak value of the EMG during MVC. Footplate moment-angle measurements and ultrasound scans were not analyzed if the EMG signal was higher than 10% of MVC (Benard et al. 2010).

Data analysis

Muscle geometry in growing children

Variables of muscle geometry were measured using an analyzing tool custom programmed in MATLAB 7.1. In this analyzing tool, the mid-longitudinal plane of GM was defined within the 3-D ultrasound array by three orientation items (Fig. 1C): (i) marker (#7) at one quarter of the distance from the most prominent dorsal point of the medial condyle to the most prominent dorsal point of the lateral femur condyle; this marker is used as an estimate of the proximal end of muscle belly, neglecting a small anatomical part curving towards the origin into the popliteal fossa; (ii) marker (#8) at the distal muscle belly end; and (iii) a line perpendicular to tangent to the distal aponeurosis in the transversal plane. This line is a good approximation of the orientation of the mid-longitudinal plane as shown in a cadaver study (Benard et al. 2009). A fourth marker (#10) was placed at the ventral intersection of the Achilles tendon and the calcaneus (Fig. 1C).

Thirteen additional markers were placed within the selected mid-longitudinal plane: five on both the distal and proximal aponeurosis, and three along the length of the fascicle that has its middle at two-thirds of the muscle belly length (Fig. 1D). A second-order polynomial was fitted through the markers of each aponeurosis and a line was fitted through the markers of the fascicle.

Using all markers, the following seven muscle geometrical variables were calculated:

1. *musclebelly length* ℓ_m being the distance between the estimated origin and most distal end of GM muscle belly (#7 and #8, Fig. 1C);
2. *muscletendon length* ℓ_t being the distance between the most distal end of GM belly and the intersection of the tendon at the calcaneus (#8 and #10, Fig. 1C);
3. *musclefascicle length* $\ell_{(fasc)}$ as the distance between the intersections of the fitted fascicle line with the fitted polynomials of the aponeuroses (Fig. 1D);
4. *fascicleangle with the aponeurosis* $\gamma_{(fasc)}$ being the mean of (a) the angle between the fascicle line and the tangent of the polynomial at the intersection with the distal polynomial and (b) the angle between the fascicle line and the tangent of the polynomial at the intersection with the proximal polynomial (Fig. 1D);
5. *musclethickness* $\ell_{(m.th)}$ being the mean of the distances between the distal and the proximal aponeurosis polynomials, (a) measured perpendicular to the tangent of the distal aponeurosis polynomial at the intersection of the fascicle line and (b) measured perpendicular to the tangent of the proximal aponeurosis polynomial at the intersection of the fascicle line (Fig. 1D, double arrows);
6. *aponeurosislength* ℓ_a, calculated as the longest side of the selected mid-longitudinal plane modelled as a parallelogram (using ℓ_m, $\ell_{(fasc)}$ and $\gamma_{(fasc)}$; Fig. 1E);
7. lengthcomponent of the physiological cross-section $\ell_{Af} = \ell_a \cdot \sin(\gamma_{(fasc)})$ (Fig 1E; see also van der Linden et al. 1998); note that ℓ_{Af} is the sum of all fibre diameters within the mid-longitudinal plane.

The whole analysis was repeated five times, and means were calculated for all geometrical variables. A pilot study showed that with more than five repetitive measurements, standard deviations of the variables within each individual did not decrease and were < 5% of the mean for length variables and < 10% for $\gamma_{(fasc)}$.

A valid comparison of the geometrical muscle characteristics over the range of ages requires examination of the geometry at a similar reference length. Preferably, this reference would be the optimum length of the muscle (i.e. the length at which the muscle exerts its maximal active force). For adults, the joint configuration at which ankle plantar flexors attain their optimum length occurs between 10° plantar flexion and 20° dorsal flexion (Marsh et al. 1982, Maganaris, 2003). For children, this particular joint angle is unknown, nor is it known whether this angle changes with age. As the passive force of different types of

in situ rat and mice muscles (maximally dissected) starts to increase near its optimum length (cf. Jaspers et al. 1999; Williams & Goldspink, 1978; Woittiez et al. 1989; Zuurbier & Huijing, 1991), the slack length may also be an appropriate length for the comparison of the muscle geometry, provided the material properties of the muscle fibres are similar throughout development. Using the dynamometer, we determined the neutral footplate angle at which the net moment applied to the torque wrench equalled zero (φ_{neutr}) and assumed that the muscle length at this angle approaches slack length. As mechanical properties of the agonists and antagonists crossing the ankle probably develop in a similar way, the relative muscle length at φ_{neutr} (i.e. the length of the muscle with respect to optimum or slack) is assumed to be similar over the different ages, allowing a comparison of the geometrical characteristics.

Comparison of human and rat GM geometry during growth

Comparison of our data of human GM geometry with those of rats (based on values derived from the literature) is only valid at the same relative age. Therefore, we normalized the age of rats and humans with respect to their mean life expectancy (156 weeks and 80 years, respectively) and GM geometry variables with respect to initial values (i.e. measured at 6.5% of the mean life expectancy). Based on the studies of Huijing and coworkers (i.e. De Koning et al. 1987; Heslinga & Huijing, 1990, 1993; Heslinga et al. 1995), we calculated the normalized changes in geometrical variables of rat GM at its optimum length and compared these with data collected in the present study.

Statistics

Student's *t*-test was used to test for significant differences between: (i) females and males regarding age, body mass, $\ell_{(tib)}$, Achilles tendon moment arm length, φ_{neutr}, φ_{dors}, φ_{plant}, m_{dors}, m_{plant}, ℓ_m, ℓ_t, ℓ_a, ℓ_{Af}, $\ell_{(fasc)}$, $\ell_{(m.th)}$ and $\gamma_{(fasc)}$ and; (ii) left and right legs regarding all these parameters except age and body mass.

Pearson's correlation coefficients were calculated between age and these variables and between $\ell_{(tib)}$ and these variables. A least-squares fit was used to determine slope and intercept of the regression function relating age and the different variables. A Student's *t* cumulative distribution function was used to test for significant differences between females and males regarding the intercept and slope of the regression functions of the variables with age.

Generalized estimating equations (GEE, SPSS, version 17.0.1; SPSS Inc.) were used on ℓ_m, ℓ_t, ℓ_a, ℓ_{Af}, $\ell_{(fasc)}$, $\ell_{(m.th)}$ and $\gamma_{(fasc)}$ to test for main effects of moment, age and their interaction. GEE is a regression technique that enables analysis of repeated measures of one factor (i.e. footplate angle at given moment). Age was treated as a covariate. A Wald test (SPSS 17.0.1) was performed to test for significant main effects of the factors age and footplate angle and for interaction between these factors. For all statistics, the level of significance was set at $P < 0.05$. The standard deviation over subjects is reported below.

Results

The age of the subjects ranged from 5 to 12 years and the mean ages of boys and girls were similar (8.8 ± 2.8 vs. 9.1 ± 1.8, Table 1).

Effects of growth on anthropometric variables

Mean body mass, tibia length and Achilles tendon moment arm length all increased significantly with age ($r > 0.77$, Table 1). The mean values of these variables were similar between boys and girls, as were their slopes as a function of age, except for the slope of the relation between Achilles tendon moment arm and age, which was significantly higher in the boys (0.25 vs. 0.13 cm per year; Fig. 2A–C). There were no differences between the left and right leg concerning tibia length and Achilles tendon moment arm

Table 1 Mean anthropometrics and mean joint variables and their correlations with age.

	Mean (SD)		Coefficient of correlation *r*	
Variable	♀	♂	♀	♂
Age (years)	9.13 (1.82)	8.79 (2.78)	–	–
Body mass (kg)	33.81 (8.77)	31.57 (9.39)	0.77*	0.92*
$\ell_{(tib)}$ (cm)	32.30 (4.59)	31.73 (4.57)	0.82*	0.93*
AT moment arm length (cm)	3.96 (0.65)	4.38 (0.43)	0.77‡*	0.89*
φ_{neutr} (°)	−3.68 (7.52)	−5.94 (5.57)	0.02	−0.12
φ_{dors} (°)	20.43 (8.74)	20.69 (6.46)	−0.32	−0.60*
φ_{plant} (°)	−53.89 (6.86)	−51.47 (7.48)	0.46	0.57*
m_{dors} (Nm per degree)	0.17 (0.04)	0.16 (0.04)	0.52*	0.54*
m_{plant} (Nm per degree)	0.08 (0.01)	0.09 (0.02)	0.37	0.67*

$\ell_{(tib)}$, tibia length; AT, Achilles tendon; φ, footplate angle measured at 0 Nm $_{(neutr)}$, 4 Nm $_{(dors)}$ and −4 Nm $_{(plant)}$; *m*, slope of the moment-angle curve towards dorsal flexion $_{(dors)}$ and towards plantar flexion $_{(plant)}$.
*Significant correlation ($P < 0.05$).
‡Significantly different from ♂ ($P < 0.05$).

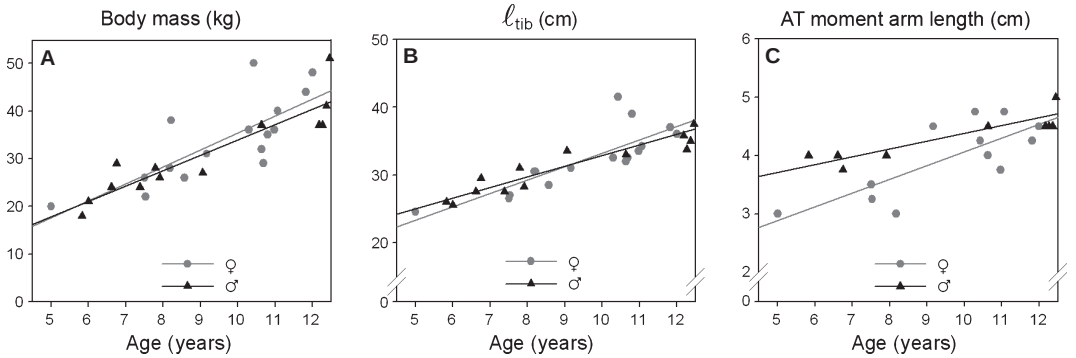

Fig. 2 Effects of growth on anthropometric variables in boys and girls. (A) Body mass, (B) tibia length ($\ell_{(tib)}$), and (C) Achilles tendon (AT) moment arm length. Regression lines are shown for boys and girls separately. Only the relationship of the AT moment arm and age was significantly different between boys and girls.

length. Body mass and tibia length increased by 3.5 kg and 1.8 cm per year, respectively, which is at different normalized rates; with respect to their initial value they increased by 18 vs. 7% per year. The normalized rate of increase of Achilles tendon moment arm length as a function of age was 6% per year.

It is concluded that for boys and girls the anthropometrics were similar except for the Achilles tendon moment arm. As expected, body mass increased at a significantly higher normalized rate compared to tibia length.

Effects of growth on ankle joint variables

Figure 3A,B shows typical examples of mean footplate moment-angle curves in the youngest and the oldest children (i.e. 5–6 vs. 11–12 years). From young to old, the angles measured at –4 and +4° Nm (i.e. φ_{plant} and φ_{dors}) decreased by approximately 11° and 16°, respectively, which amounts to a decrease of 25 and 40%, respectively. In boys, both footplate angles φ_{plant} and φ_{dors} correlated significantly with age (Table 1). In girls, the correlation coefficients for both φ_{plant} and φ_{dors} with age had the same sign as for boys, but these correlations were not significant. Note that for girls, this is explained by outlying data (Fig. 3E). The footplate angle measured at 0 Nm (φ_{neutr}) was similar for boys and girls and did not change with age (Table 1, Fig. 3D). There was no difference between left and right legs regarding joint parameters.

The unchanged neutral angle and the reduction of both φ_{plant} and φ_{dors} resulted in increased slopes m_{plant} and m_{dors} in older children (Fig. 3F–G). For boys and girls, the slopes increased by 0.02 and 0.07 Nm per degree, respectively (i.e. 36 and 55%). This indicates that functional characteristics in boys and girls developed in a similar way and that the range of motion (ROM) of angular foot movement, measured at standardized moments, decreases with age. The increased slopes of the moment-angle curves indicate that stiffness of angular foot movement increases with age.

Effects of growth on variables of muscle geometry and their acute changes as a function of footplate angle

Muscle geometry of GM changed considerably during growth in both boys and girls. As there were no differences between boys and girls, muscle geometrical variables were pooled across gender. There was no difference between left and right legs regarding muscle geometry.

Generalized estimating equations (GEE) showed significant effects of age for all variables except $\gamma_{(fasc)}$. All length variables increased with age, which is confirmed by their correlations with age (Fig. 4). Muscle length (ℓ_m) increased 1 cm (i.e. 6%) per year. Tendon length (ℓ_t) grew at a rate of 8% (or 0.9 cm per year), i.e. similar to that of the muscle belly and aponeurosis. The muscle-tendon complex ($\ell_m + \ell_t$) increased 1.9 cm (i.e. 7%) per year. Aponeurosis length (ℓ_a) and fascicle length ($\ell_{(fasc)}$) increased at different absolute rates but at similar rates when normalized to initial length (i.e. 0.8 and 0.2 cm, or 7 and 5%, per year, respectively). The length component of the physiological cross-section (ℓ_{Af}) increased 9% per year (not shown), indicating that GM muscle length also increased due to trophy. Note that the full length of GM tendinous tissues (i.e. $\ell_a + \ell_t$) increased at a similar rate of 7%, indicating that there was no change in the length ratio of the tendinous parts located inside and outside the muscle belly.

As $\gamma_{(fasc)}$ did not change significantly for the age range studied, we conclude that growth-related increases in ℓ_m are fully explained by increases of ℓ_a (related to fibre trophy) and $\ell_{(fasc)}$ (Fig. 5), with changes in ℓ_a contributing 80% of the increase in muscle length and changes in $\ell_{(fasc)}$ contributing 20%.

After normalization of all muscle-related length variables with respect to tibia length, no correlation with age was present, indicating that tibia length is a more important factor for all these length variables.

GEE showed significant main effects of footplate angle (at given moments) for all variables (Fig. 4). Wald tests

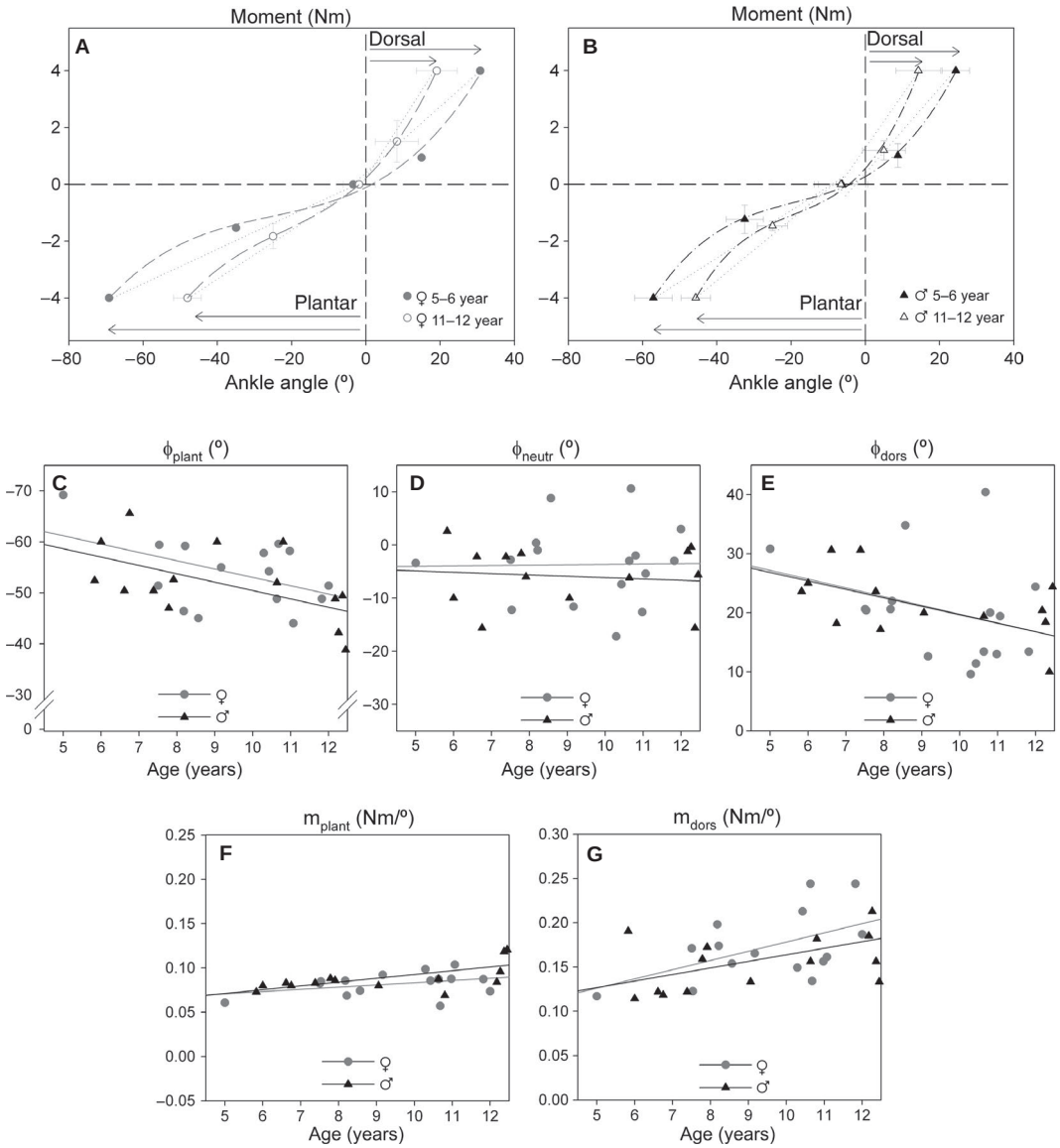

Fig. 3 Footplate moment-angle curves for the youngest and oldest group and the effects of growth on joint-related variables. Footplate moment-angle curves for the youngest and oldest group: (A) girls, and (B) boys. Mean (and SD) footplate angles and moments are shown for the 5–6 year age group and the 11–12 year age group. The curves are third-order polynomials fitted to the moment-angle data. There was no difference in neutral footplate angle, measured at 0 Nm, between both groups. For the 11–12-year age group, ROM (arrows) were smaller and the estimated slopes (dotted lines) were significantly higher towards both plantar flexion and dorsal flexion. Footplate joint-related variables: (C) footplate angle towards plantar flexion at −4 Nm (φ_{plant}), (D) footplate angle at 0 Nm (φ_{neutr}), (E) footplate angle towards dorsal flexion at 4 Nm (φ_{dors}), (F) slope of the moment-angle curve for plantar flexion (m_{plant}), and (G) slope of the moment-angle curve for dorsal flexion (m_{dors}). Individual values are plotted for both boys and girls.

showed for all ages that acutely changing the footplate angle from φ_{neutr} to φ_{dors} increased ℓ_m and $\ell_{(fasc)}$ (respectively +13 and +15%) but did not affect ℓ_t, ℓ_a, $\ell_{(m.th)}$ or $\gamma_{(fasc)}$. Lengthening of GM by footplate rotation is thus caused mostly by elongation of its fascicles. Wald tests also showed that with footplate movement over the ROM from φ_{plant} to φ_{dors}, muscle thickness ($\ell_{(m.th)}$) increased substantially (+10%). Elongation of the muscle belly over the total ROM increased $\ell_{(fasc)}$ and decreased $\gamma_{(fasc)}$.

GEE showed no significant interaction between the factors age and footplate angle for ℓ_m, ℓ_t, $\ell_{(m.th)}$ or $\gamma_{(fasc)}$. Therefore, the regression lines of the respective graphs (Fig. 4A,B,E,F) should be considered to be parallel, indicating that the acute absolute changes in these variables as a function of footplate angle were similar at different ages. In contrast, significant interaction effects were found for $\ell_{(fasc)}$ and ℓ_a. Wald tests showed that for $\ell_{(fasc)}$, the slope at φ_{dors} was higher than that at either φ_{plant} or φ_{neutr} (Fig. 4C).

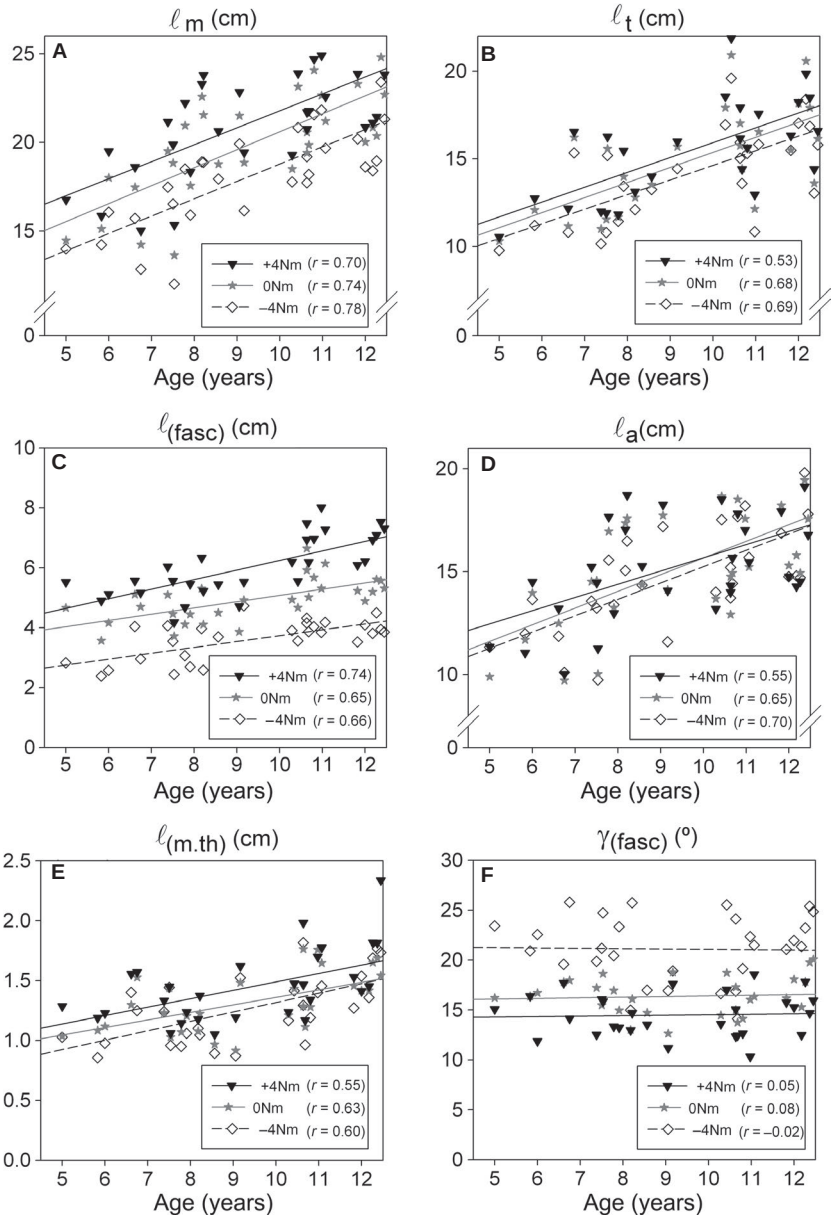

Fig. 4 Effects of growth on variables of muscle geometry measured at different footplate moments. (A) Muscle belly length (ℓ_m), (B) tendon length (ℓ_t), (C) fascicle length ($\ell_{(fasc)}$), (D) aponeurosis length (ℓ_a), (E) muscle thickness ($\ell_{(m.th)}$), and (F) fascicle–aponeurosis angle ($\gamma_{(fasc)}$) all plotted as a function of age. All variables were measured in GM for three conditions (i.e. –4 Nm, 0 Nm and +4 Nm applied to the footplate). For the regression analysis, the data on both genders were pooled, as there was no significant difference between boys and girls. Statistical analysis with GEE (factors age and footplate moment-angle) showed significant main effects of age for all muscle geometry variables (with the notable exception of $\gamma_{(fasc)}$). For all variables, the coefficient of correlation *r* with age is shown for the three moment conditions.

For ℓ_a, the opposite was found; the slope at φ_{dors} was lower than that at φ_{plant} and φ_{neutr} (Fig. 4D). This difference in the response of $\ell_{(fasc)}$ and ℓ_a to acute GM elongation indicates that at older age the aponeuroses become stiffer, and therefore with acute GM elongation more length change is needed from its fascicles.

Effects of growth on anthropometric and geometrical variables: children vs. young rats

In children and in rats, from an age of 6–10% of life expectancy (i.e. 5–8 years in children and 10–16 weeks in rats), body mass and tibia length grew at similar rates (Fig. 6A–B). This is also true for GM belly length, which grew proportionally with increases in tibia length (Fig. 6C). For children, the ratio of GM muscle belly length (at neutral footplate angle) and tibia length was 0.63 and did not change with age (Fig. 6E). In young rats, at GM optimum length, this ratio was about 0.89 and also did not change with age. It is concluded that for growing rats, normalized GM muscle belly was about 43% longer than for children. This relatively long muscle belly in rats is accompanied by relatively long aponeurosis and fascicles (i.e. $\ell_a/\ell_{(tib)}$ and $\ell_{(fasc)}/\ell_{(tib)}$ were respectively 0.6 and 0.3 in rats vs. 0.4 and 0.2 in children). Fascicle length in the children, but not in rats, was shown to increase with age (Fig. 6D). Also, the normalized length component of the physiological cross-section was higher in rats (0.24 in rats vs. 0.11 in children, Fig. 6F) but both variables increased by similar percentages (42% in rats and 41% in children).

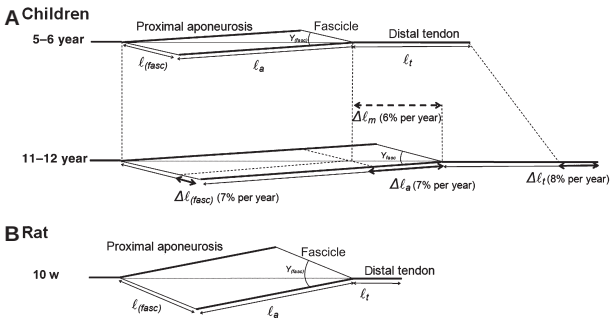

Fig. 5 Schematic representation of normalized muscle geometry of GM in young children and in young rats. (A) In GM of children, ℓ_a and $\ell_{(fasc)}$ increase by 7% per year from the younger to the older group. This results in an increase of muscle belly length ($\Delta\ell_m$) at a similar rate. The increase in ℓ_a has the largest absolute contribution to $\Delta\ell_m$. Note that $\gamma_{(fasc)}$ does not differ between groups. (B) GM mid-longitudinal plane geometry of young rats (age = 10 weeks) is shown with the muscle length (ℓ_m) scaled to ℓ_m of young children. In rats, normalized $\ell_{(fasc)}$ and $\gamma_{(fasc)}$ are both higher compared to those of GM of the children. The normalized Achilles tendon length is substantially smaller compared to that of children.

In contrast, fascicle angle with the aponeurosis in rat GM was substantially larger than in GM of children (26° vs. 16°).

The ratio between Achilles tendon length and tibia length was more than three times greater in children than in rats (i.e. 0.37 vs. 0.11, respectively).

Discussion

GM geometry in children was studied using 3-D ultrasound imaging. A major finding was that during human growth between the ages of 5 and 12 years, GM increased its length proportionally with the increased tibia length by uniform scaling: the length component of the physiological cross-sectional area of GM as well as GM fascicles both increased in length, without changes of fascicle angle with the aponeurosis. GM geometry in the children was not affected by gender.

GM growth of children differs from that of rats. In rat GM, muscle belly length increases exclusively by an increase in physiological cross-sectional area and does not scale uniformly. Although the contribution of growing fascicle length to the increase in muscle belly length is small compared with that of the length component of the physiological area in human GM (20 vs. 80%), we have to reject the hypothesis that GM muscle belly in children grows in length exclusively by an increase in the length component of the physiological area.

Geometrical changes in human GM during growth

In parallel fibred muscle and muscle with a very low degree of pennation (i.e. lines of pull of muscle fibres and of the muscle being almost parallel), growing muscle can only increase its length by adding sarcomeres in series, i.e. by increasing fibre and fascicle length. In more highly pennate muscle (such as GM) additional factors need to be considered. To date, very little is known about the geometrical changes in skeletal muscle in children. The few studies investigating muscle development in children examined geometric variables separately. Recalculating the results from 2-D ultrasound studies of GM (Mohagheghi et al. 2008) we estimate that fascicle length would increase by 4% per year and that over 20 years, muscle thickness and fascicle angle (data Binzoni et al. 2001) would increase by about 7 and 5% per year, respectively. We found similar values for fascicle length and muscle thickness. In contrast, for the age range of 5–12 years, based on results of Binzoni et al., a sizable increase is expected ($\Delta\gamma_{(fasc)} = 10°$ per year), but we found no significant changes in fascicle angle with the aponeurosis. This is explained by a sizeable inter-individual variation contributing to the size of the standard deviation. However, if there had been an actual increase, our data shows it would have been limited to 0.3° per year. Based on our findings we conclude that, for the ages 5–12 years, fascicle angle will only increase very slightly, at best. In mammals, the number of muscle fibres may increase in the very early period immediately after birth (first months). However, during later growth an increase in physiological cross-sectional area has been shown to be primarily the result of muscle fibre hypertrophy rather than muscle fiber hyperplasia (cf. for review Goldspink, 1972; Pearson, 1990; Antonio & Gonyea, 1993). Increases in fascicle angle will therefore create room for the increased component of muscle fibre diameter along the aponeurosis (for an explanation of this process, see also Rollhäuser & Wendt, 1955). If fascicle angle hardly changes, this implies that the expected increase in fibre and fascicle diameters within GM can only be accommodated by a simultaneous and proportional increase in aponeurosis length. These considerations indicate that GM longitudinal growth in children between the ages of 5 and 12 years is the result of growth of its muscle fibres and fascicles in both length and in diameter, the latter contributing most.

Comparison of growth-related geometrical changes in human and rat GM and mechanisms underlying regulation of GM geometry

Results for growth of human GM differ from those reported for rat GM. For similar normalized ranges of age in rats, muscle longitudinal growth of GM occurs exclusively by growth in the diameter of its muscle fibres and fascicles (i.e. in rats, GM fascicle length does not increase). This discrepancy suggests fundamental differences in the regulation of GM growth between both humans and rats.

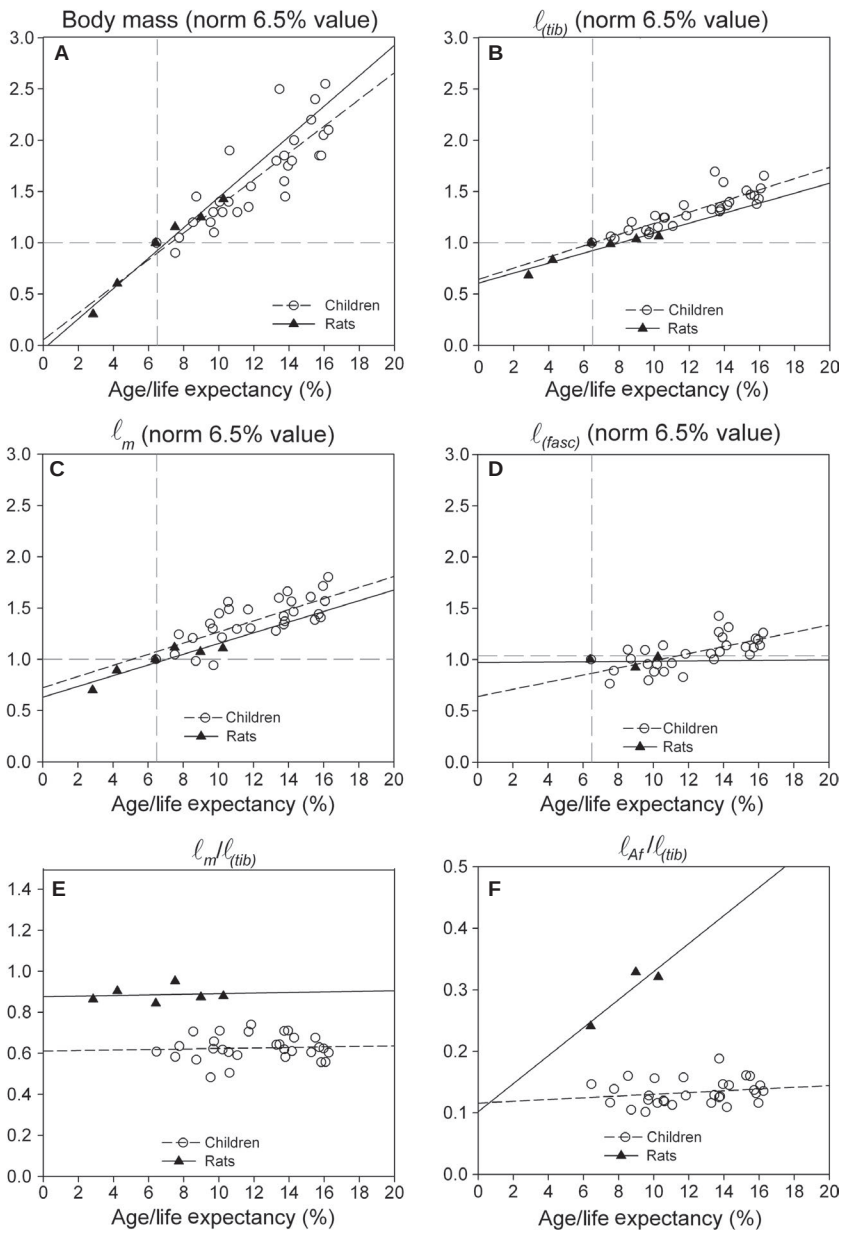

Fig. 6 Comparison of effects of growth in young rats and children. (A) Normalized body mass. (B) Normalized tibia length ($\ell_{(tib)}$). (C) Normalized muscle (belly) length (ℓ_m). (D) Normalized fascicle length ($\ell_{(fasc)}$). (E) Ratio of muscle (belly) length and tibia length ($\ell_m/\ell_{(tib)}$). (F) Ratio of the length component of the physiological cross-sectional area and tibia length ($\ell_{Af}/\ell_{(tib)}$). Age is normalized for respective values of life expectancy. Body mass and length variables (A–D) are normalized for their initial value (at intercept, i.e. at normalized age of 6.5%). Data on the rats were obtained from De Koning et al. (1987), Heslinga & Huijing (1990, 1993) and Heslinga et al. (1995) and reanalyzed.

We have shown that at 6.5% of expected lifespan, GM muscle belly length normalized for tibia length in rat was 143% of that in human. Consequently, the relative tendon length of GM was significantly smaller in rats. The relatively long muscle belly in rats was accompanied by higher normalized fascicle and aponeurosis lengths as well as a 10° higher fascicle angle with the aponeurosis (Fig. 5B). Consequently, in rats the normalized length component of the physiological cross-section within the GM mid-longitudinal plane (ℓ_{Af}) was also higher (by 140%). Such a difference in ℓ_{Af} may be caused not only by a relatively larger fascicle diameter, but also may be the result of having relatively more muscle fibres arranged parallel with the longitudinal direction of the muscle. The impact of differences in GM geometry between rats and humans on how this muscle grows is considerable and raises the question of which mechanisms underlie the differences in growth of geometric variables of rodents and humans. These mechanisms may be related to: (i) changes in the required functional demands (maximum force and length) applied to the muscle during development, (ii) endocrine factors, or (iii) change in muscle excursion during development.

We have shown that the rate of increase in length component of the physiological cross-section (ℓ_{Af}) of GM normalized for tibia length was similar in rats and children, which is likely due to similar normalized rates of fibre diameter growth. This similarity may imply similar functional demands during growth. However, as rats are quadrupeds, as well as toe-walkers, the net result of these conditions on the demand for GM muscle force is difficult to predict. In

addition, differential changes in rat and human GM geometry during growth may be explained by growth factor signalling during development. Recently, studies using *ex vivo* culture of mature isolated muscle fibres, showed that muscle anabolic growth factors induce radial muscle fibre growth (trophy) without longitudinal growth (Jaspers et al. 2008; Watt et al. 2010). For rat GM, trophy-induced gains in muscle length will be large enough to attain optimum length at the joint angle at which a muscle is most frequently active (Huijing & Woittiez, 1984). For human GM, the magnitude of trophy-induced muscle length gain is smaller due to the smaller fascicle angle. Therefore, serial addition of sarcomeres is required to maintain proportionality between GM optimum length and tibia length.

Furthermore, muscle excursion could potentially be a stimulus for growth of GM in children (e.g. Crawford, 1954). The rationale for this is that during normal growth, the increase in the moment arm leads to an increase in muscle length over the full joint ROM and an increase in serial sarcomere number would accommodate that need. For rodents, muscle excursion does not seem to be a regulating factor of serial sarcomere number (cf. Huijing & Jaspers, 2005). However, this may be different for growing children. The Achilles tendon moment arm increases with age, whereas the range of footplate angles during walking remains constant (Stansfield et al. 2001). Consequently, the length range over which GM actually exerts force will be increased during gait, which may stimulate longitudinal growth of GM. Further research is warranted to determine to what extent the stimuli of body growth and muscle excursion contribute to how GM grows in children.

Functional implications of GM growth on ROM of angular foot movement and GM extensibility

Growth-related changes

Our present finding of a decreasing ROM towards footplate dorsal flexion (at 4 Nm) by about 1.5° per year, is in accordance with a decrease of about 2° per year estimated from data of a study on joint laxity in Chinese children of the similar age range (Cheng et al. 1991). Such a decrease in ROM with normal growth has been ascribed to changes within joint capsules, ligaments and muscle-tendon complexes (e.g. Cheng et al. 1991; Gajdosik et al. 1999). However, how much each of these structures contributes to limiting ROM is unknown. GM contributes to passive ankle stiffness: passive ankle stiffness in adults measured with the knee extended (long gastrocnemius) is 20–40% higher than with knee flexed (short gastrocnemius) (Riemann et al. 2001).

Within skeletal muscle, structures contributing to passive joint resistance are: (i) intracellularly: cross-linking between the actin and myosin filaments in passive muscle fibres, generating a tension without EMG activity and filaments such as titin (Wang et al. 1993), and (ii) extracellularly: connective tissues such as endomysia, perimysia and epimysia (see for review Gajdosik, 2001). At present, we show that with normal body growth, increasing length of GM occurs to a great extent by trophy of its fascicles. With more muscle tissue arranged in parallel, resistance to lengthening of GM will be higher. Note that in children, increases in muscle tissue arranged in series (i.e. number of sarcomeres) with normal growth of GM also affects ROM (i.e. increase). As the contribution of increase in fascicle length to muscle belly was four times smaller than that of the increase in the length component of the physiological cross-section, the effect of added serial muscle tissue on ROM will also be small. Therefore, the added parallel muscle tissue is expected to have the largest effect on ROM.

Changes in tendon length accompanying angular foot movement

Our present results show that, in children, elongation of GM lengthened its fascicles, whereas tendon and aponeurosis length were minimally affected. Several studies of GM in adults yielded opposite conclusions with respect to tendon elongation (cf. Abellaneda et al. 2009; Herbert et al. 2002; Kawakami et al. 2008; Morse et al. 2008a): on passive ankle movement towards dorsal flexion, elongation of the tendon has been shown to be considerable (i.e. 27–53%). These differences may be explained by different techniques for measuring GM tendon length. In our study, GM tendon length was measured directly in the 3-D reconstruction of GM, whereas in the studies mentioned above, GM tendon length change was calculated indirectly by subtracting muscle belly length change from muscle tendon complex change calculated from ankle angles (Grieve et al. 1978). In addition, there are differences in externally applied moments: approximately 4 Nm in the children in our study vs. $\geq$ 20 Nm in the adults in the cited references (not reported in Herbert et al. 2002). With a greater moment applied to the ankle, it is likely that a greater force will be exerted on the passive structures of GM, which will be lengthened more. As applying 4 Nm, exerted with the hand-held dynamometer, was close to the maximum moment the children could tolerate without discomfort, we were not able to measure GM elongation at larger moments. A third possible explanation may be that at higher age, due to an increase in physiological cross-sectional area (i.e. more tissue in parallel), GM muscle belly becomes stiffer, necessitating greater tendon length change.

Changes in GM muscle thickness accompanying angular foot movement

Our present results show that after lengthening of GM, its thickness was increased. Although we are not the first to report such a phenomenon (cf. Legerlotz et al. 2010), this increase is remarkable. As the volume of the muscle is constant, it was expected that with elongation, muscle thickness would decrease somewhat. Such a decrease of

thickness has been found with elongation of *in situ* rat GM (e.g. Huijing & Woittiez, 1984). However, in that study, GM was exposed and maximally dissected from its surrounding tissues, leaving it free of forces exerted by these tissues. In the present study, human GM, studied *in vivo*, was connected to all of its surrounding tissues. With additional external forces exerted on GM, effects of elongation on its deformation are difficult to predict. Our present data show that the effects of an increase in fascicle length outweigh the effects of a decrease in fascicle angle on muscle thickness, yielding a net increase in muscle thickness. Contrary to the rat *in situ* study, forces exerted on GM by movement of the foot are not necessarily aligned with the longitudinal direction of GM. For example, if the foot is dorsally flexed from the 0° footplate angle, the insertion of the Achilles tendon on the calcaneus will move caudally but also ventrally, exerting forces on GM in similar directions. As a result, GM becomes longer with angular movement of the foot, but also thicker. Note that we measured GM thickness at two-thirds of muscle belly length. However, by studying the contours of GM we have the impression that this also occurred more proximal to this location. Muscle thickness cannot be measured adequately more distal to the two-thirds location because the most distal fascicles cannot be distinguished from the proximal aponeurosis at the intersection.

Footplate movement towards plantar flexion

ROM towards plantar flexion has been investigated less frequently than dorsal flexion. Limitations of ROM towards plantar flexion constitute fewer problems clinically in walking, for example, where dorsal flexion is an absolute prerequisite for foot clearance and a stable stance phase (Rose & Gamble, 1994) and decreases of plantar flexion may only limit push off, which can be compensated in many ways. Furthermore, during walking, older children will experience greater active and/or passive forces (due to higher body mass or because of higher forces generated by antagonistic muscles) and therefore the range of motion through gait may not be affected. However, studying plantar flexion ROM may contribute to understanding of total ankle ROM. Our present results indicate that during normal growth, ROM towards plantar flexion (at 4 Nm) decreased by 4% per year. This decrease could be caused by changes in the properties of the dorsal flexors similar to those found in GM. In addition, in rodents, myofascial connections between antagonistic muscle groups have been shown to be present (for a review see Huijing, 2009), specifically between m. triceps surae and dorsal flexors of the ankle (e.g. Meijer et al. 2007; Rijkelijkhuizen et al. 2007). This means that forces generated actively or passively within antagonistic muscle may be exerted at the tendon of an agonistic muscle. If this is the case, to understand limits to passive ROM of a joint one needs to consider the properties of the directly stretched muscle, as well as its antagonistic muscles. Therefore, observed geometrical changes in GM with normal growth potentially also contribute to decreasing plantar flexion ROM, but also vice versa (e.g. the dorsal flexor muscles affecting dorsal flexion ROM).

We conclude that decreased dorsal flexion ROM at a given joint moment in older children is explained by an increased length component of the physiological area of GM with normal growth. Fascicles of GM are likely opposing factors to elongation of GM in children and stiffness measured at the ankle is largely determined by the stiffness of GM fascicles (muscle fibres and intermuscular connective tissues). This may be true for ankle dorsal flexor muscles as well, as the plantar flexion also decreases with age.

Limitations of this study

Some limitations of our study need to be taken into account:

1 We studied children in late infancy and pre-adolescence (5–12 years). Our data indicate linear relationships for the variables investigated. It is unlikely that during early infancy and puberty the studied variables will change linearly and therefore extrapolation from our conclusions to a different age range should be performed with extreme care.
2 The images obtained using 3-D ultrasound have a lower resolution than images obtained with 2-D ultrasound. However, the resolution of 3-D ultrasound images is sufficient for visualizing fascicles. Furthermore, the advantage of 3-D ultrasound is that the mid-longitudinal plane can be found in a standardized manner post-experimentally, avoiding errors of measurement in geometrical variables (Benard et al. 2009) and measurements can be performed within a much larger region (i.e. muscle belly and tendon length) compared to 2-D ultrasound images.
3 We have reported the moments applied at the interface between torque wrench and foot fixation. Ideally, one would like to know the net moment at the talocrural joint to relate to gastrocnemius data. However, this net moment can only be estimated globally using mean data from the literature, concerning foot mass, as well as foot size, in addition to the known apparatus mass. All such factors affect the net ankle moment. Using moment balance equations for the foot, foot-fixation and torque wrench as one free-body, it was calculated that for the dorsal flexion condition the estimated ankle moment differs most from the external moment actually exerted (i.e. by +1.9 Nm). This results in a maximum difference in footplate angle of less than 5°, causing differences in muscle–tendon complex length and muscle fascicle length of about 1%. Therefore, these effects of weight, as well as those of different foot size, were neglected and we chose to report the measured externally applied

moment on the footplate rather than the estimated net moment at the talocrural joint.

4 We studied GM and drew inferences about externally applied moment. However, other parts of m. triceps surae and antagonistic muscles contribute to this moment. We can therefore only speculate about quantitative changes in this moment as the result of changes of GM geometry with normal growth. It is likely that muscle volume of other ankle plantar flexors and antagonistic muscles will also increase with growth, influencing this moment.

5 Fascicle-related variables (length and angle) were studied only at one location within GM muscle belly. This involves an implicit assumption of homogeneity. However, detailed anatomical and physiological study of GM showed distributions (even within the mid-longitudinal plane, and larger distribution within the whole muscle) of fascicle length and angle and of the serial number of sarcomeres, as well as the mean sarcomere length of fibre (e.g. Huijing, 1985; Dekhuijzen et al. 1986; Zuurbier & Huijing, 1992; Jaspers et al. 1999). Nonetheless, our present measurements of fascicle length and angle are representative of a large group of fascicles within the mid-longitudinal plane. Despite that, we feel that the current results under the assumption of homogeneity constitute a first step in understanding how GM geometry changes with normal growth. For obvious reasons, measurement of serial sarcomere number is impossible in human subjects. How the effects of inhomogeneity of fibre length, serial sacromere number and fibre mean sarcomeres lengths will affect the relation between geometrical parameters and the mechanical properties of GM should be an object of further research.

Concluding remarks

We have studied GM development and ROM of angular foot movement in children aged 5–12 years using a novel combination of 3-D ultrasound imaging technique and hand-held dynamometry. The 3-D ultrasound imaging technique allows measurement of geometrical variables in a standardized manner in the mid-longitudinal plane of GM. GM growth in children was compared with that of rats.

For growing children, we show that the geometry of GM and its tendon scales uniformly with length. The length component of the physiological cross-section as well as the fascicle length increased with age, whereas the fascicle angle did not change. Between 5 and 12 years, GM geometry develops similarly in boys and girls. ROM of angular foot movement towards dorsal flexion decreases during growth, which is explained by the uniform scaling of the GM geometry.

The combined knowledge regarding the development of GM geometry, ROM of angular foot movement and accompanying stiffness provides a reference set for studying muscle pathology of children with neuromuscular disorders and for input of neuromuscular models studying effects of muscle growth and pathology on movement control. As 3-D ultrasound imaging allows for measurements of gross muscle geometry, studying highly pennate muscles such as GM in growing children with muscle pathology will enhance our knowledge of the effects of such diseases and of intervention with, for example, pharmacological denervation, casting and soft tissue surgery.

Acknowledgements

This study was funded by the Phelps Stichting voor Spastici, Bussum, the Netherlands. We are very grateful to Adam Shortland and Nicola Fry at Guy's Hospital London for their help with 3-D ultrasound imaging in the pre-project phase and for allowing us their algorithms for the construction of the 3-D voxel array, to be implemented in our MATLAB programs. We are very grateful to José Maas and Idsart Kingma for their help with the moment–balance equations concerning net ankle moment.

Author contributions

M. R. Bénard: acquisition of data, data analysis/interpretation, contributions to concept/design, drafting of the manuscript, critical revision of the manuscript, approval of the article. J. Harlaar and J. G. Becher: data interpretation, contributions to concept/design, critical revision of the manuscript, approval of the article. P. A. Huijing and R. T. Jaspers: data interpretation, contributions to concept/design, drafting of the manuscript, critical revision of the manuscript, approval of the article.

References

Abellaneda S, Guissard N, Duchateau J (2009) The relative lengthening of the myotendinous structures in the medial gastrocnemius during passive stretching differs among individuals. *J Appl Physiol* **106**, 169–177.

Antonio J, Gonyea WJ (1993) Skeletal muscle fiber hyperplasia. *Med Sci Sports Exerc* **25**, 1333–1345.

Barber L, Barrett R, Lichtwark G (2009) Validation of a freehand 3D ultrasound system for morphological measures of the medial gastrocnemius muscle. *J Biomech* **42**, 1313–1319.

Benard MR, Becher JG, Harlaar J, et al. (2009) Anatomical information is needed in ultrasound imaging of muscle to avoid potentially substantial errors in measurement of muscle geometry. *Muscle Nerve* **39**, 652–665.

Benard MR, Jaspers RT, Huijing PA, et al. (2010) Reproducibility of hand-held ankle dynamometry to measure altered ankle moment-angle characteristics in children with spastic cerebral palsy. *Clin Biomech (Bristol, Avon)* **25**, 802–808.

Binzoni T, Bianchi S, Hanquinet S, et al. (2001) Human gastrocnemius medialis pennation angle as a function of age: from newborn to the elderly. *J Physiol Anthropol Appl Human Sci* **20**, 293–298.

Blazevich AJ, Sharp NC (2005) Understanding muscle architectural adaptation: macro- and micro-level research. *Cells Tissues Organs* **181**, 1–10.

Cheng JC, Chan PS, Hui PW (1991) Joint laxity in children. *J Pediatr Orthop* **11**, 752–756.

Crawford GN (1954) An experimental study of muscle growth in the rabbit. *J Bone Joint Surg Br* **36-B**, 294–303.

De Koning JJ, van der Molen HF, Woittiez RD, et al. (1987) Functional characteristics of rat gastrocnemius and tibialis anterior muscles during growth. *J Morphol* **194**, 75–84.

Dekhuijzen AJ, van Koetsveld PA, Baan GC, et al. (1986) Motor endplate position of rat gastrocnemius muscle. *Muscle Nerve* **9**, 642–647.

Freriks B, Hermens H, Disselhorst-Klug C, et al. (1999) The recommendations for sensors and sensor placement procedures for surface electromyography. In *SENIAM 8; European Recommendations for Surface Electromyography* (eds Hermens H, Freriks B, Merletti R, et al.), pp. 13–54. Enschede: Roessingh Research and Development B.V.

Fry NR, Gough M, Shortland AP (2004) Three-dimensional realisation of muscle morphology and architecture using ultrasound. *Gait Posture* **20**, 177–182.

Gajdosik RL (2001) Passive extensibility of skeletal muscle: review of the literature with clinical implications. *Clin Biomech (Bristol, Avon)* **16**, 87–101.

Gajdosik RL, Vander Linden DW, Williams AK (1999) Influence of age on length and passive elastic stiffness characteristics of the calf muscle-tendon unit of women. *Phys Ther* **79**, 827–838.

Gee A, Prager R, Treece G, et al. (2004) Processing and visualizing three-dimensional ultrasound data. *Br J Radiol* **77** (Spec No. 2), S186–S193.

Goldspink G (1972) Postembryonic growth and differentiation of striated muscle. In *The Structure and Function of Muscle* (ed. Bourne GH), pp. 179–236. Atlanta: Academic Press.

Grieve W, Pheasant S, Cavanagh PR (1978) Prediction of gastrocnemius length from knee and ankle joint posture. In *Biomechanics VI-A, International Series on Biomechanics* (eds Asmussen E, Jorgensen K), pp. 405–412. Baltimore: University Park Press.

Herbert RD, Moseley AM, Butler JE, et al. (2002) Change in length of relaxed muscle fascicles and tendons with knee and ankle movement in humans. *J Physiol* **539**, 637–645.

Heslinga JW, Huijing PA (1990) Effects of growth on architecture and functional characteristics of adult rat gastrocnemius muscle. *J Morphol* **206**, 119–132.

Heslinga JW, Huijing PA (1993) Muscle length-force characteristics in relation to muscle architecture: a bilateral study of gastrocnemius medialis muscles of unilaterally immobilized rats. *Eur J Appl Physiol Occup Physiol* **66**, 289–298.

Heslinga JW, te Kronnie G, Huijing PA (1995) Growth and immobilization effects on sarcomeres: a comparison between gastrocnemius and soleus muscles of the adult rat. *Eur J Appl Physiol Occup Physiol* **70**, 49–57.

Huijing PA (1985) Architecture of the human gastrocnemius muscle and some functional consequences. *Acta Anat* **123**, 101–107.

Huijing PA (2009) Epimuscular myofascial force transmission: a historical review and implications for new research. International society of biomechanics Muybridge award lecture, Taipei, 2007. *J Biomech* **42**, 9–21.

Huijing PA, Jaspers RT (2005) Adaptation of muscle size and myofascial force transmission: a review and some new experimental results. *Scand J Med Sci Sports* **15**, 349–380.

Huijing PA, Woittiez RD (1984) The effect of architecture on skeletal muscle performance: a simple planimetric model. *Neth J Zool* **34**, 21–32.

Jaspers RT, Brunner R, Pel JJ, et al. (1999) Acute effects of intramuscular aponeurotomy on rat gastrocnemius medialis: force transmission, muscle force and sarcomere length. *J Biomech* **32**, 71–79.

Jaspers RT, van Beek-Harmsen BJ, Blankenstein MA, et al. (2008) Hypertrophy of mature Xenopus muscle fibres in culture induced by synergy of albumin and insulin. *Pflugers Arch* **457**, 161–170.

Kawakami Y, Abe T, Fukunaga T (1993) Muscle-fiber pennation angles are greater in hypertrophied than in normal muscles. *J Appl Physiol* **74**, 2740–2744.

Kawakami Y, Abe T, Kanehisa H, et al. (2006) Human skeletal muscle size and architecture: variability and interdependence. *Am J Hum Biol* **18**, 845–848.

Kawakami Y, Kanehisa H, Fukunaga T (2008) The relationship between passive ankle plantar flexion joint torque and gastrocnemius muscle and Achilles tendon stiffness: implications for flexibility. *J Orthop Sports Phys Ther* **38**, 269–276.

Kurihara T, Oda T, Chino K, et al. (2005) Use of three-dimensional ultrasonography for the analysis of the fascicle length of human gastrocnemius muscle during contractions. *Int J Sport Health Sci* **3**, 226–234.

Legerlotz K, Smith HK, Hing WA (2010) Variation and reliability of ultrasonographic quantification of the architecture of the medial gastrocnemius muscle in young children. *Clin Physiol Funct Imaging* **30**, 198–205.

van der Linden BJ, Koopman HF, Grootenboer HJ, et al. (1998) Modelling functional effects of muscle geometry. *J Electromyogr Kinesiol* **8**, 101–109.

Mademli L, Arampatzis A (2008) Mechanical and morphological properties of the triceps surae muscle-tendon unit in old and young adults and their interaction with a submaximal fatiguing contraction. *J Electromyogr Kinesiol* **18**, 89–98.

Maganaris CN (2003) Force-length characteristics of the in vivo human gastrocnemius muscle. *Clin Anat* **16**, 215–223.

Marsh E, Sale D, Quinlan J, et al. (1982) Influence of joint position on ankle plantarflexion in humans. *J Appl Physiol* **52**, 1636–1642.

Meijer HJ, Rijkelijkhuizen JM, Huijing PA (2007) Myofascial force transmission between antagonistic rat lower limb muscles: effects of single muscle or muscle group lengthening. *J Electromyogr Kinesiol* **17**, 698–707.

Mohagheghi AA, Khan T, Meadows TH, et al. (2008) In vivo gastrocnemius muscle fascicle length in children with and without diplegic cerebral palsy. *Dev Med Child Neurol* **50**, 44–50.

Morse CI, Degens H, Seynnes OR, et al. (2008a) The acute effect of stretching on the passive stiffness of the human gastrocnemius muscle tendon unit. *J Physiol* **586**, 97–106.

Morse CI, Tolfrey K, Thom JM, et al. (2008b) Gastrocnemius muscle specific force in boys and men. *J Appl Physiol* **104**, 469–474.

Narici MV, Maganaris CN, Reeves ND, et al. (2003) Effect of aging on human muscle architecture. *J Appl Physiol* **95**, 2229–2234.

Pearson AM (1990) Muscle growth and exercise. *Crit Rev Food Sci Nutr* **29**, 167–196.

Prager RW, Rohling RN, Gee AH, et al. (1998) Rapid calibration for 3-D freehand ultrasound. *Ultrasound Med Biol* **24**, 855–869.

Riemann BL, DeMont RG, Ryu K, et al. (2001) The effects of sex, joint angle, and the gastrocnemius muscle on passive ankle joint complex stiffness. *J Athl Train* **36**, 369–375.

Rijkelijkhuizen JM, Meijer HJ, Baan GC, et al. (2007) Myofascial force transmission also occurs between antagonistic muscles located within opposite compartments of the rat lower hind limb. *J Electromyogr Kinesiol* **17**, 690–697.

Rollhäuser H, Wendt GG (1955) Zur innern Mechanik des hypertrophischen Muskels. *Morphologie* **95**, 151–161.

Rose J, Gamble JG (1994) *Human Walking*. Baltimore: Williams & Wilkins.

Shortland AP, Harris CA, Gough M, et al. (2002) Architecture of the medial gastrocnemius in children with spastic diplegia. *Dev Med Child Neurol* **44**, 158–163.

Stansfield BW, Hillman SJ, Hazlewood ME, et al. (2001) Sagittal joint kinematics, moments, and powers are predominantly characterized by speed of progression, not age, in normal children. *J Pediatr Orthop* **21**, 403–411.

Stickland NC (1983) Growth and development of muscle fibres in the rainbow trout (*Salmo gairdneri*). *J Anat* **137**(Pt 2), 323–333.

Tardieu C, Huet de la Tour E, Bret MD, et al. (1982) Muscle hypoextensibility in children with cerebral palsy: I. Clinical and experimental observations. *Arch Phys Med Rehabil* **63**, 97–102.

Thom JM, Morse CI, Birch KM, et al. (2007) Influence of muscle architecture on the torque and power-velocity characteristics of young and elderly men. *Eur J Appl Physiol* **100**, 613–619.

Van Gelein Vitringa VM, Jaspers R, Mullender M, et al. (2011) Early effects of muscle atrophy on shoulder joint development in infants with unilateral birth brachial plexus injury. *Dev Med Child Neurol* **53**, 173–178.

Wang K, McCarter R, Wright J, et al. (1993) Viscoelasticity of the sarcomere matrix of skeletal muscles. The titin-myosin composite filament is a dual-stage molecular spring. *Biophys J* **64**, 1161–1177.

Watt KI, Jaspers RT, Atherton P, et al. (2010) SB431542 treatment promotes the hypertrophy of skeletal muscle fibers but decreases specific force. *Muscle Nerve* **41**, 624–629.

Williams PE, Goldspink G (1978) Changes in sarcomere length and physiological properties in immobilized muscle. *J Anat* **127**, 459–468.

Woittiez RD, Heerkens YF, Huijing PA, et al. (1989) Growth of medial gastrocnemius muscle and Achilles tendon in Wistar rats. *Anat Anz* **168**, 371–380.

Zuurbier CJ, Huijing PA (1991) Influence of muscle shortening on the geometry of gastrocnemius medialis muscle of the rat. *Acta Anat (Basel)* **140**, 297–303.

Zuurbier CJ, Huijing PA (1992) Influence of muscle geometry on shortening speed of fibre, aponeurosis and muscle. *J Biomech* **25**, 1017–1026.